Smith, S. O., Pardoen, J. A., Mulder, P. P. J., Curry, B., Lugtenburg, J., & Mathies, R. (1983) *Biochemistry 22*, 6141–6148.
Spiess, H. (1979) in *Dynamic NMR Spectroscopy*, pp 55–214, Springer-Verlag, Berlin, Heidelberg, and New York.
Stockburger, M., Klusmann, W., Gattermann, H., Massig, G., & Peters, R. (1979) *Biochemistry 18*, 4886–4900.
Tegenfeldt, J., & Haeberlen, U. (1979) *J. Magn. Reson. 36*, 453–457.
Tokito, Y., Inoue, Y., Chujo, R., & Miyoshi, Y. (1975) *Org. Magn. Reson. 7*, 485–487.
Trewhella, J., Anderson, S., Fox, R., Gogol, E., Khan, S., Engelman, D., & Zaccai, G. (1983) *Biophys. J. 42*, 233–241.
Wolff, E. K., Griffin, R. G., & Waugh, J. S. (1977) *J. Chem. Phys. 67*, 2387–2388.
Yamaguchi, A., Unemoto, T., & Ikegami, A. (1981) *Photochem. Photobiol. 33*, 511–516.

Differential Light Scattering and Absorption Flattening Optical Effects Are Minimal in the Circular Dichroism Spectra of Small Unilamellar Vesicles†

David Mao and B. A. Wallace*

ABSTRACT: The large size of membrane particles and the high local concentration of proteins in these particles give rise to differential scattering and absorption flattening effects which result in significant distortions of the circular dichroism spectra of membrane proteins and produce erroneous estimates of secondary structure. In an attempt to find a membrane system in which scattering and flattening are minimal, but in which native protein conformation is retained, several methods of fragmentation, including sonication, solubilization, and incorporation into small unilamellar vesicles (SUVs), were examined. Bacteriorhodopsin in purple membrane sheets was used as a test system for the effectiveness of the procedures since its secondary structure is known from independent physical measurements and these large membranes produce considerable distortions, as seen by comparison of observed and calculated spectra for the protein. While sonication decreased differential scattering, it had little effect on the total distortion; solubilization in octyl glucoside tended to decrease both differential scattering and flattening but induced some conformational change in the protein. However, when bacteriorhodopsin was incorporated into small unilamellar vesicles, which both decrease particle size and dilute the local concentration of protein, the spectrum produced was nearly identical with the calculated one, suggesting that SUVs may be appropriate vehicles for use with membrane proteins and may be a facile method for eliminating optical artifacts.

The circular dichroism (CD)[1] spectra of particulate samples such as membrane suspensions are distorted by the optical artifacts of differential light scattering (Bustamante et al., 1983) and differential absorption flattening (Gordon & Holzwarth, 1971; Duysens, 1956). These distortions must be removed in order to analyze the data accurately.

Differential light scattering is the difference in the extent of scattering of left and right circularly polarized light by an optically active sample, which will be detected by a spectropolarimeter as if it were differential absorption and leads to distortion of the protein spectrum. The inherent difference in the indices of refraction for left and right circularly polarized light exhibited by an optically active particle is the primary source of this differential scattering. Results of differential light scattering are abnormally large or small CD peaks, a dependence of the CD spectrum on the detector acceptance angle, and CD signals outside the absorption range of the chromophore. The angular dependence and the magnitude of differentially scattered intensities are functions of the particle size and relative orientation and distance between the scattering units within each particle (Bustamante et al., 1983).

A complete correction for differential scattering is potentially possible by using fluorescence-detected circular dichroism (FDCD), which permits measurement with an effective acceptance angle of 4 sr (Reich et al., 1980). Alternatively, if the scattering is concentrated in the forward direction, as is the case for spherical particles, an end-window photomultiplier detector placed directly behind the sample cell should also be sufficient to collect most of the scattered light (Schneider & Harmatz, 1976).

Absorption flattening occurs when chromophores are closely packed, resulting in a smaller total physical cross-sectional area than if the molecules were uniformly dispersed. Consequently, the probability for protein molecules to encounter photons is decreased, and the protein absorption is correspondingly reduced. The extent of flattening is a function of the size of the particles and the concentration of chromophores within each particle.

An optically active particulate sample will exhibit differential flattening of the absorption of the left and right circularly polarized light because chiral particles absorb oppositely polarized light differently. Because the degree of flattening is directly proportional to absorption, the reduction in the CD signal varies with the wavelength and is maximal at wavelengths corresponding to absorption peaks. Consequently, a significant distortion in the shape of the CD spectrum may result.

† From the Department of Biochemistry and Molecular Biophysics, Columbia University, New York, New York 10032. *Received November 21, 1983.* This work was supported by Grant GM-27292 from the National Institutes of Health. B.A.W. is the recipient of a Hirschl Career Scientist Award.

[1] Abbreviations: BR, bacteriorhodopsin; PM, purple membrane; DMPC, dimyristoylphosphatidylcholine; SUV, small unilamellar vesicle; NOG, *n*-octyl glucoside; SDS, sodium dodecyl sulfate; CD, circular dichroism; FDCD, fluorescence-detected circular dichroism.

0006-2960/84/0423-2667$01.50/0

Differential flattening cannot be eliminated instrumentally, as can differential scattering. The correction factors for absorption flattening could be calculated if one had precise information on the shape of the particle, the protein density distribution within the particles, and the intrinsic absorption of each protein molecule (Gordon & Holzwarth, 1971). Such an approach is not generally feasible, however, because of the difficulties in determining the physical parameters required for the calculation. However, it should be possible to remove the differential flattening experimentally, if one could place the protein molecules in a phospholipid bilayer environment which does not exhibit significant scattering and in which the proteins are maximally dispersed.

In order to test the success of any such procedure, one needs as a test system a membrane protein whose secondary structure has been determined by independent means. Since the secondary structures of few membrane proteins are known, the choice of systems is limited. One such protein is the light-driven proton pump bacteriorhodopsin (BR), which is the sole protein component in the single-bilayer sheets of purple membranes (PMs) from *Halobacteria halobium* (Oesterhelt & Stoeckenius, 1971). Since BR associates into two-dimensional hexagonal lattices of trimers in the purple membrane, its three-dimensional structure has been determined to 7-Å resolution by electron diffraction and image reconstruction (Henderson & Unwin, 1975). Each BR molecule appears to contain seven transmembrane α-helices which comprise about 80% of the polypeptide chain (Engelman et al., 1980). The strong axial reflections at 1.5 and 5 Å in the X-ray diffraction pattern of PMs also indicate an abundance of transmembrane helices (Henderson, 1975). Hence, this may be a good test system. Furthermore, the large dimensions (5000–10000 Å) and high protein concentration (75% by weight) of the PM patches give rise to significant differential light scattering and absorption flattening effects which produce a considerable distortion in the CD spectrum of this molecule.

This study has examined the effects of different methods of fragmentation and dispersion on differential scattering and flattening. The secondary structures of BR in sonicated membrane fragments, in detergent micelles, and in small unilamellar vesicles (SUVs) have been compared with the calculated spectrum of BR derived from diffraction data in order to determine if any of these environments are suitable for spectroscopic studies of native membrane proteins.

Materials and Methods

Dimyristoylphosphatidylcholine (DMPC) was obtained from Calbiochem, and *n*-octyl glucoside (NOG) was from Sigma. Spectrum wet cellulose dialysis tubing with a molecular weight cutoff of 25000 was used. *Halobacteria halobium*, strain S9, was grown, and purple membranes were isolated as previously described (Oesterhelt & Stockenius, 1971).

The BR concentration in dark-adapted purple membrane samples was determined by using a molar extinction coefficient of 63000 at 568 nm (Rehorek & Heyn, 1979). The BR concentration in DMPC vesicles was determined by the method of Lowry et al. (1951) in the presence of 0.1% SDS with dark-adapted PM as the standard. However, the very high concentration of lipid in these samples tends to affect the assay, giving spuriously high values, which lead to inappropriately low calculated ellipticities. Hence, the normalization factors (see CD Data Analysis) may be the most accurate indicators of concentration for the vesicle samples. Lipid concentrations were determined by a modified Fiske–Subbarow phosphate assay (Fiske & Subbarow, 1925), using hydrogen peroxide to oxidize the organic compounds.

Sample Preparations. PMs were washed with either deionized water or 0.15 M KCl by repeated centrifugation at 4 °C for 15 min at 30900*g*. PM samples were solubilized according to the procedure of Dencher of Heyn (1978): 795 μL of a PM suspension (0.31 mg of BR/mL) in deionized water was mixed with 205 μL of 6% *n*-octyl glucoside (NOG) in deionized water to give a sample of 0.25 mg of BR/mL (9.3 μM) and 1.23% NOG (41 mM). The samples were placed in the dark at 23 °C for 24 h and then incubated at 7 °C for an additional 24 h.

In order to prepare small purple membrane patches, 600 μL of a suspension of PM (0.30 mg of BR/mL) in deionized water was sonicated at 4 °C using 10-s bursts with a Soniprep microprobe ultrasonicator for a total of 90 s.

To prepare BR–DMPC vesicles, 1.0 mg of DMPC in $CHCl_3$–MeOH (2:1) was dried under nitrogen and then under vacuum. A solution of 500 μL of PM (0.24 mg of BR) in 0.15 M KCl was added to the dried lipid. An initial lipid:protein ratio (w/w) of 4:1 (mole ratio = 153) was used. The resulting suspension was sonicated with the microprobe using 20-s bursts for 3 min at 37 °C. Samples were then desalted by dialysis against two changes of 6 L of deionized water at 22 °C for 24 h. Near-complete removal of KCl was verified by the absence of precipitate in the presence of 0.1% SDS. The KCl was removed because it interferes with absorption measurements below 200 nm and precipitates the SDS which is added later to solubilize the vesicles. The BR–DMPC vesicle sample was sonicated for 1 min with the microprobe and dialyzed for another 24 h. Some vesicles were solubilized by the addition of 1 μL of 10% SDS to 99 μL of the vesicle sample.

Spectroscopy. CD spectra were recorded on a Cary 60 spectropolarimeter fitted with a Model 6001 CD attachment and a variable position detector. The wavelength range scanned was 300–190 nm. The instrument was calibrated with *d*(+)-10-camphorsulfonic acid at 290 nm. The calibration at lower wavelengths was checked with sperm whale myoglobin. Detector acceptance angles ranging from 90° to 2° were achieved by translating the end-window photomultiplier tube detector along the optical axis and by varying the phototube aperture (Schneider & Harmatz, 1976).

Measurements of the CD spectra were routinely made at 27 °C by using a 0.5- or a 0.1-mm path-length cell. In general, a scanning speed of 5 nm/min and a time constant of 3 s were used. The spectra reported are the average of three or four scans measured every 1 nm. For PM samples, blank runs of deionized water were subtracted from the appropriate sample spectra. For vesicle samples, DMPC vesicles without protein were used as blanks. For samples which contained detergent, the same amount of detergent was also added to the blanks.

Electron Microscopy. Samples were placed on Formvar- or carbon-coated copper grids and stained with 0.5% or 1% aqueous uranyl acetate for 15 s. The grids were examined in either a JEOL 200 or a Philips 300 electron microscope.

CD Data Analysis. Data points were analyzed at 1-nm intervals between 190 and 240 nm by both linear, unconstrained (Magar, 1968), and nonlinear, constrained (Himmelblau, 1972), least-squares curve-fitting procedures to obtain estimates of each type of secondary structure present in the sample. The constrained least-squares fit required that the fraction of each conformation be positive but did not require that the sum of the fractions be unity. The reference data set for the analysis was derived from 15 water-soluble proteins (Chang et al., 1978). An average helix length of 26 was used in the analysis since this value approximates the length of α-helix necessary to span the purple membrane bilayer

(Henderson & Unwin, 1975; Engelman et al., 1980).

The results were normalized to 100% by dividing each fraction by the sum of the fractions in order to remove variations due to concentration errors (Mao et al., 1982). The quality of each computed fit was evaluated by calculating a normalized root mean square deviation (NRMSD) for each curve (Brahms & Brahms, 1980), as given by

$$\text{NRMSD} = \left[\frac{\sum_N (\theta_{\text{exptl}} - \theta_{\text{calcd}})^2}{\sum_N \theta_{\text{exptl}}^2} \right]^{1/2}$$

where θ_{exptl} and θ_{calcd} are experimental and calculated mean residue ellipticities, respectively, and N is the number of data points used.

Results and Discussion

Unconstrained linear least-squares analyses of the experimental CD data were initially done. If negative coefficients were obtained in the unconstrained analysis, the analysis was considered unsuccessful, and a constrained least-squares analysis was then done to produce results which make physical sense (e.e., no fractions less than zero). Because of possible errors in protein concentrations, the sum of the fractions of the secondary structures was not required to be unity, as this constraint would result in large distortions of the structural fractions calculated (Mao et al., 1982; Hennessey & Johnson, 1982). Since the magnitudes of the reported CD spectra of PM differ significantly, depending on how the concentration was determined (Jap et al., 1983; Long et al., 1977; Reynolds & Stoeckenius, 1977), this suggests that determinations of BR concentration may not be precise and that any constrained solution which relies on the absolute concentration would be in error. The normalization of the structural fractions corrects for protein concentration error; it does not change the relative proportions of secondary structures calculated from the data (Mao et al., 1982; Mao, 1984). The correspondence between the calculated and experimental CD spectra was measured by the NRMSD. For soluble proteins, NRMSD values less than 0.1 indicate a close match between the calculated and experimental CD curves and generally indicate a good correspondence with the X-ray structure (Brahms & Brahms, 1980). Small NRMSD values, however, do not necessarily mean that the calculated structures resemble the actual structures; the use of reference spectra that do not reflect the structures present in the protein would not result in an accurate determination of secondary structures (Baker & Eisenberg, 1976). Similar arguments also apply to another algorithm used to calculate secondary structures (Provencher & Glöckner, 1981). Since the latter method of calculation may be even more biased by a single aberrant protein in the reference data set, it was not used for these analyses.

Purple Membranes. The secondary structure of BR in PM, estimated from electron microscopic and diffraction data and model-building studies, is approximately 80% α-helix, 10% β-turn, and 10% random coil. Myoglobin, a water-soluble monomeric protein, is similarly composed of 80% α-helix, as determined by X-ray diffraction (Kendrew et al., 1960; Kendrew, 1962), and can be used for comparison as a dispersed system which does not exhibit differential scattering and flattening. The measured spectrum of myoglobin and the calculated spectrum of BR, on the basis of diffraction data (Figure 1), serve as indicators of the effectiveness of the procedures employed to remove the optical artifacts.

The CD spectrum of BR in purple membrane sheets (Figure 1) does not resemble the CD spectrum of myoglobin in magnitude or shape, nor does it agree with the predicted CD spectrum for BR. In order to determine the extent of the distortion that is due to differential light scattering, spectra were measured with different detector acceptance angles. As the acceptance angle of the detector decreased from 90° to 2°, the peaks in the 190–210- and 220–240-nm regions of the PM CD spectrum increased in magnitude and shifted toward longer wavelengths (Figure 2). These acceptance angle dependent changes suggest that PMs do exhibit some differential light scattering. However, while the difference between the 90° and 2° spectra is significant, the differences from the 90° spectrum drop off rapidly with increasing angle, indicating that most of the scatter is in the near-forward direction. This is confirmed by the similarity of the 90° spectrum and the published FDCD (360°) spectrum of PM (Jap et al., 1983) and suggests that differential light scattering is not a significant factor in the CD spectra of membranes obtained by using large

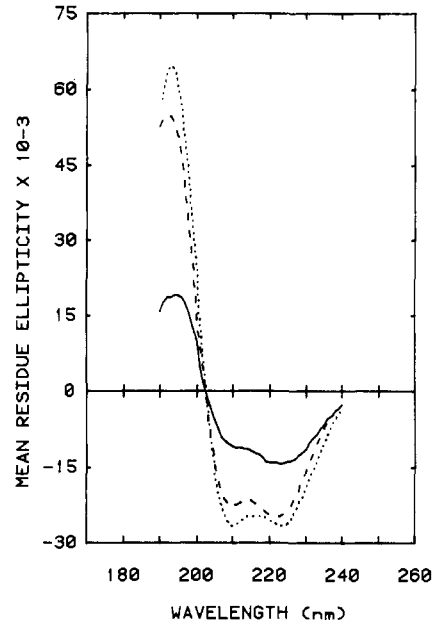

FIGURE 1: Measured CD spectra of bacteriorhodopsin in purple membrane sheets (—) and of whale myoglobin (- - -), plus the calculated spectrum for bacteriorhodopsin based on a secondary structure of 80% α-helix, 10% β-turn, and 10% random coil (···).

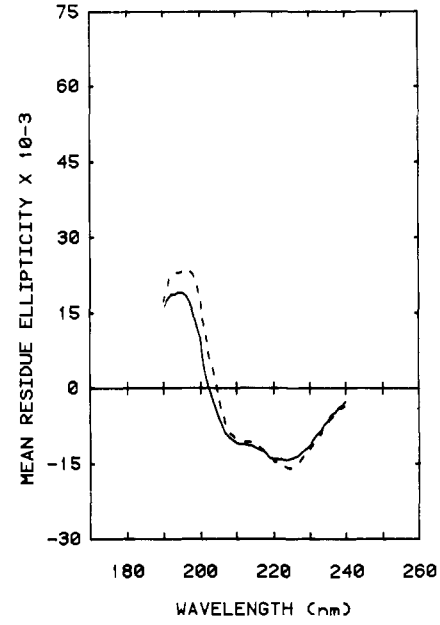

FIGURE 2: CD spectra of bacteriorhodopsin in purple membrane sheets obtained with detector acceptance angles of 90° (—) and 2° (- - -).

Table I: Calculated Secondary Structures[a]

sample	unconstrained					constrained				
	α	β	T	R	NMRSD	α	β	T	R	NMRSD
intact purple membrane	0.51	−0.55	0.36	0.28	0.127	0.45	0.00	0.26	0.29	0.157
sonicated membranes	0.54	−0.59	0.31	0.11	0.132	0.62	0.00	0.25	0.13	0.159
octyl glucoside solubilized membranes	0.41	−0.10	0.14	0.19	0.071	0.56	0.00	0.17	0.27	0.073
BR–DMPC vesicles	0.83	0.05	0.05	0.07	0.036	*b*	*b*	*b*	*b*	*b*
SDS-solubilized BR–DMPC vesicles	0.37	0.24	−0.01	0.21	0.062	0.47	0.25	0.00	0.27	0.062
pseudo-reference-state-corrected data[c]	0.36	1.30	−0.38	0.11	0.073	0.54	0.25	0.00	0.21	0.128

[a] Solutions with only positive coefficients are reported as normalized values. Abbreviations: α, α-helix; β, β-sheet; T, β-turn; R, random coil. [b] Unconstrained fits unnecessary (all values positive). [c] From Long et al. (1977).

acceptance angles, in contrast to the case for other large particles such as bacteriophages (Bustamente et al., 1983). Differential absorption flattening must then be the major factor producing the distortion of the CD spectrum of PM. Even though protein molecules are uniformly distributed within the purple membranes and the membranes are randomly dispersed in solution, the proteins are sequestered in membrane patches, which comprise a relatively small portion of the total volume of the solution; for such a chromophore distribution, the Beer–Lambert relationship does not hold. The result is an apparent reduction in the absorption, which is most pronounced at wavelengths where the absorbance is highest: the 197- and 210-nm peaks in the PM spectrum are depressed more than the 224-nm peak with respect to those peaks in the calculated BR spectrum.

An unconstrained least-squares analysis of the PM data produced poor results (NRMSD much greater than 0.1), and the calculated amount of α-helical structure was only 50%, with a large negative amount of β-sheet structure (Table I). Variation of the average length of the α-helical segments over a range from 10 to 30 amino acids did not significantly improve either the fit or the proportions of secondary structures. The constrained least-squares analysis produced an α-helical content of less than 50% (Table I), which is clearly at odds with the diffraction data.

These results indicate that differential flattening significantly affects the CD analysis of BR in PMs. Therefore, in order to obtain a undistorted spectrum of BR, it will be necessary to examine BR under conditions where the molecules are relatively uniformly dispersed in a membrane environment in which they maintain their native conformation.

Sonication. Since sonication reduces the maximum dimension of the PM sheets to ~250 Å without disrupting the two-dimensional lattice of BR molecules or reducing the BR concentration within each membrane, this procedure is expected to have a significant effect on light scattering. The reduction in differential light scattering is evident from the diminished effect of different detector acceptance angles on the CD spectra of sonicated PM samples (data not shown). However, since the differential light scattering effect is insignificant in the CD spectrum of even intact PM collected with an acceptance angle of 90°, the reduction in particle size of PM patches by sonication is not expected to greatly affect the CD spectrum measured with this acceptance angle. Sonication does not change the concentration of proteins within each membrane fragment but does decrease the particle size and the absorption of each particle. This is expected to slightly reduce the dampening effect in the low-wavelength region of the spectrum, where absorption flattening is most significant.

After sonication, the magnitude and shape of the CD spectrum of the membrane patches still did not match either the calculated BR spectrum or the myoglobin spectrum. When compared to the CD spectrum of native PM, the sonicated

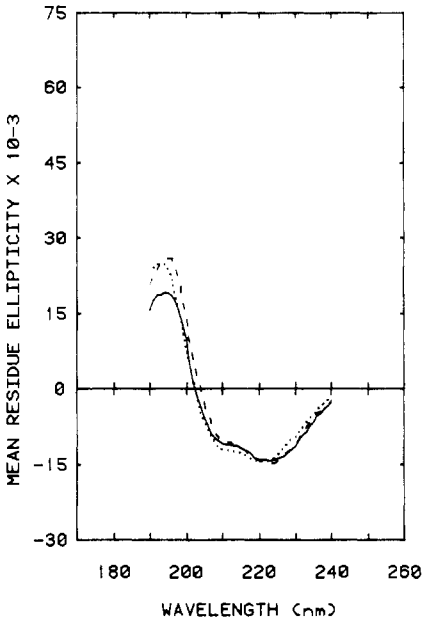

FIGURE 3: CD spectra of intact (—), sonicated (---), and octyl glucoside solubilized (···) purple membrane sheets, all obtained with detector acceptance angles of 90°.

sample exhibited approximately a 25% increase in ellipticity in the 190–197-nm range (Figure 3), although no significant changes were detected in the rest of spectrum. The increase in ellipticity at low wavelengths is most likely due to the decrease in differential flattening but could also be due to a conformational change in BR induced by the sonication, although the change, which corresponds to an increase in helix content (Table I), is a rather unlikely consequence of denaturation.

Inappropriately small α-helix and large negative β-sheet structural fractions were calculated for this sample (Table I). The NRMSD for the fit was large (0.132) and similiar to that of native PM. The constrained fit also produced an α-helical content significantly lower than that expected for BR (Table I). These poor results suggest that other methods which more effectively reduce absorption flattening need to be examined.

Detergent Solubilization. Treatment of PM with detergent disperses the BR molecules into small micelles, thereby reducing both the scattering and absorption flattening. It has been reported that BR is solubilized into "monomeric" forms in both Triton X-100 and NOG (Dencher & Heyn, 1978). Upon solubilization in NOG, the mean residue ellipticity at 195 nm increased relative to that at 224 nm, leading to a slight change in the shape of the CD spectrum (Figure 3). The shape of the solubilized PM CD spectrum was more similar to the myoglobin spectrum and the predicted BR spectrum, and the parameters calculated from the unconstrained least-squares fit were significantly better for the solubilized sample than for intact sheets. The NRMSD was reduced to 0.07, and the

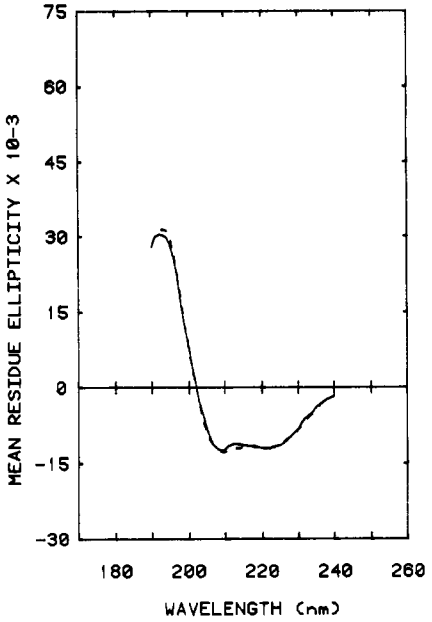

FIGURE 4: CD spectra of bacteriorhodopsin in DMPC vesicles obtained with detector acceptance angles of 90° (—) and 8° (---).

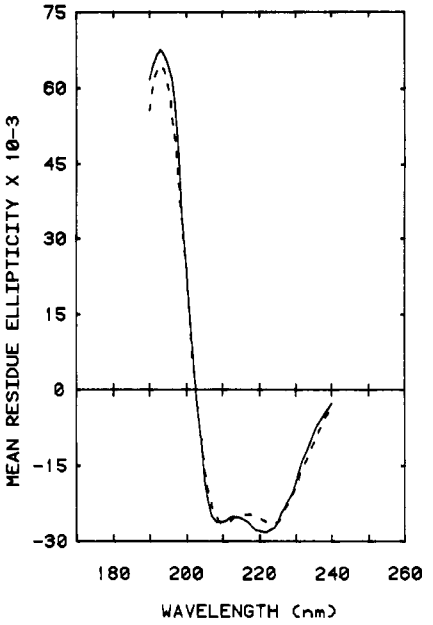

FIGURE 5: Comparison of the normalized bacteriorhodopsin spectrum in DMPC vesicles (—) and the calculated spectrum (---) based on diffraction data.

amount of β-sheet calculated was only slightly negative (Table I). However, the proportion of α-helical structure was still less than 50%. Constrained fits only increased the α-helix content to 56% (Table I), a value comparable to the 61% detected by Dencher & Heyn (1978). Similiar results were obtained for Triton X-100 solubilized PM (Jap et al., 1983). The proportions of α-helix calculated for BR in these detergents may not correspond to those in the native protein, however, because the presence of detergent may change the protein conformation. The large shift (>20 nm) observed in the absorbance peak of the retinal chromophore accompanying solubilization suggests that the protein structure is indeed altered by this procedure. Solubilization with SDS tends to reduce the α-helical content even further (Table I); this treatment results in extensive denaturation of the protein, as indicated by the >100-nm shift in the retinal absorption peak. Hence, although detergent solubilization serves to remove differential scattering and flattening effects, it does not appear to provide an environment sufficiently similar to phospholipid bilayers to maintain the native protein structure.

Small Unilamellar Vesicles. An alternate manner of dispersing the BR molecules is to package them in SUVs. When PM is sonicated in the presence of DMPC, the hexagonal lattice is disrupted, and the BR molecules are incorporated into 300 Å diameter vesicles. This treatment reduces the differential light scattering distortion, as illustrated by the near identity of the CD spectra of BR–DMPC vesicles taken with large and small acceptance angles (Figure 4).

Incorporation into SUVs also serves to reduce absorption flattening. In the limit of one protein per vesicle, the sample would be equivalent to a dispersed solution and the absorption flattening eliminated. Since the average number of BR molecules per vesicle in this study is small (~20), the distribution of BR in DMPC vesicles approaches the degree of uniformity exhibited by a protein solution. Consequently, the normalized CD spectrum of the BR–DMPC sample closely matches the CD spectrum of myoglobin and the predicted CD spectrum of BR (Figure 5). The fractional secondary structures calculated in the unconstrained analysis were all positive for BR–DMPC vesicles and corresponded to the values derived from diffraction studies (Table I), with a very low NRMSD of 0.04.

The observed change in the CD spectrum of BR upon incorporation into vesicles cannot be attributed to the sonication process alone because the CD spectrum of PM barely changed upon sonication without DMPC present. Rotational diffusion and retinal exciton-coupling measurements (Heyn et al., 1981; Cherry et al., 1978, 1981) have indicated that BR in unilamellar DMPC vesicles is largely monomeric, provided the DMPC:BR mole ratio is greater than 80:1 and the temperature of the sample is greater than 23 °C, as it is in these specimens. It is possible that disruption of the two-dimensional lattices present in PM could cause some alteration in the structure. However, intermolecular interactions are not expected to be significant for this protein, since two crystal forms with very different molecular contacts and packing (the second form of which does not contain trimers) have nearly identical structures (Unwin & Henderson, 1975; Leifer & Henderson, 1983). Therefore, the changes in the spectrum observed upon incorporation into vesicles must be due primarily to elimination of absorption flattening, and this suggests that SUVs are appropriate vehicles for spectroscopic studies of the native protein.

Small unilamellar vesicles have a number of properties which make them suitable for spectroscopic studies: their total measured absorbance (intrinsic plus scattering) in the 190–240-nm region is small and allows collection of protein CD data to as low as 190 nm, which permits the significantly different spectral characteristics of the various secondary structures in the low-wavelength region to be used to obtain accurate fits. The rotational strengths of the electronic transitions of the ester and phosphate head groups of the phospholipids are very weak compared to those of the peptide backbone, so nearly all the signal will be due to protein. Furthermore, scattering by these small particles is minimal. One concern, however, is if different vesicle sizes are produced in the presence and absence of proteins, the scattering characteristics of the protein-containing vesicles could differ somewhat from those of pure lipid vesicles, even though the samples with and without proteins are prepared in the same manner and have equivalent lipid concentrations. In this study, the vesicles prepared with and without proteins appeared to have similar molecular dimensions, so different scattering

properties between sample and blank are not a concern.

There are a few potential disadvantages to the use of SUVs: Not all membrane proteins retain their native conformations and activities upon reconstitution, and the small size of the vesicles results in a significantly larger radius of curvature than in most natural membranes, which may interfere with the structures of some (especially large) membrane proteins. Therefore, one must have some independent measure of protein structural integrity in SUVs (e.g., retention of the retinal absorption peak for BR, or transport assays for channels). BR incorporated into DMPC vesicles by the sonication procedures used in this study exhibits high light-driven proton pumping activity (H. Rodman, V. Balogh-Nair, and B. A. Wallace, unpublished results; Racker, 1973). The BR–DMPC vesicles in this study also exhibit an absorption peak centered around 550–560 nm, which agrees with the position of retinal absorption in BR–DMPC vesicles formed by Triton X-100 or cholate dialysis procedures (Cherry et al., 1978; Lewis & Engelman, 1983) that produce vesicles capable of proton translocation with pumping kinetics similar to those of BR in PM (Dencher & Heyn, 1979; Bamberg et al., 1981). The results suggest that the dispersed BR must be very similiar in structure to BR in PM.

The use of SUVs seems to be more successful in removing the optical distortions than other methods which have been applied to correct the spectra of membrane proteins. For example, the pseudo-reference-state method (Urry. 1972) has been applied to the CD spectrum of PM (Long et al., 1977). This method requires a dispersed state (the pseudo reference state) of the protein in order to calculate correction factors, so PMs were solubilized in SDS–trifluoroethanol. From the corrected data, the authors calculated an α-helical content of 73% for BR on the basis of a single data point (224 nm). However, structural information extracted from a single data point is generally unreliable (Barela & Darnall, 1974). Furthermore, this was not a fair test since the one data point used was in the high-wavelength region of the spectrum which is less affected by light scattering and absorption flattening. Calculating the secondary structure from their corrected data at all wavelengths, we obtained a maximum α-helical content of about 54% with 25% β-sheet also present (Table I). This result is contrary to the known structure of BR. Such a poor result is not unexpected since the pseudo-reference-state method relies on the assumption that the structure of the membrane remains unaltered upon solubilization. This circumstance is unlikely in the presence of SDS, a detergent which tends to denature proteins. When BR–DMPC vesicles were solubilized in 0.1% SDS, a similarly low α-helical content and a significant β-sheet content (Table I) were obtained (47% α-helix and 25% β-sheet), suggesting that SDS does indeed cause significant structural changes in BR and that the pseudo-reference-state data may be providing information on the conformation of the molecule as found in detergents rather than as in membranes.

Another method used for membrane proteins, in which corrections are made for differential light scattering but not for absorption flattening effects, also produces poor results. Using FDCD, Jap et al. (1983) found 38% α-helix and 46% β-sheet content for bacteriorhodopsin in purple membranes. Since flattening is proportional to the absorption, it would tend to depress the 195-nm peak relative to the 224-nm peak, resulting in an underestimate of the α-helix and an overestimate of the β-sheet, which is what was observed. This result emphasizes the need for a method that will correct differential flattening as well as differential scattering.

In summary, the uncorrected CD data for BR in native purple membranes would indicate that the protein is only 50% α-helical, which is in conflict with results obtained by other physical measurements. This discrepancy is a consequence of both differential light scattering and absorption flattening effects, which must be considered and corrected for in CD studies of membrane samples. The differential scattering and flattening distortions may be minimized by using small unilamellar vesicles. A helical content of ~80% is calculated for BR in this type of sample, which corresponds well with the value derived from diffraction studies of PMs. The near-identity of the normalized CD spectrum of BR–DMPC vesicles with that of either the calculated BR spectrum or the measured myoglobin spectrum suggests that SUVs are appropriate vehicles for examination of this membrane protein by CD spectroscopy. Furthermore, a similarly close correspondence of the calculated secondary structure derived from CD with that detected by diffraction methods has also been observed for the hydrophobic plant protein crambin in SUVs (Wallace et al., 1984). These results indicate that SUVs formed *with high lipid to protein ratios* may provide an appropriate environment for spectroscopic studies of membrane proteins in which differential light scattering and absorption flattening effects are minimal.

Acknowledgments

We thank C. Teeters for helpful discussions and aid with the computer programs used for data analysis and L. Vargus and L. Re for growing the halobacteria.

Registry No. DMPC, 13699-48-4; NOG, 29836-26-8.

References

Baker, C. G., & Eisenberg, I. (1976) *Biochemistry 15*, 629–634.

Bamberg, E., Dencher, N. A., Fahr, A., & Heyn, M. P. (1981) *Proc. Natl. Acad. Sci. U.S.A. 78*, 7502–7506.

Barela, T. D., & Darnall, D. W. (1974) *Biochemistry 13*, 1694–1700.

Brahms, S., & Brahms, J. (1980) *J. Mol. Biol. 138*, 149–178.

Bustamante, C., Tinoco, I., & Maestre, M. F. (1983) *Proc. Natl. Acad. Sci. U.S.A. 80*, 3568–3572.

Chang, C. T., Wu, C.-S. C., & Yang, J. T. (1978) *Anal. Biochem. 91*, 13–31.

Cherry, R. J., & Godfrey, R. E. (1981) *Biophys. J. 36*, 257–276.

Cherry, R. J., Mueller, U., Henderson, R., & Heyn, M. P. (1978) *J. Mol. Biol. 121*, 283–298.

Dencher, N. A., & Heyn, M. P. (1978) *FEBS Lett. 96*, 322–326.

Dencher, N. A., & Heyn, M. P. (1979) *FEBS Lett. 108*, 307–310.

Duysens, L. N. M. (1956) *Biochim. Biophys. Acta 19*, 1–12.

Engelman, D. M., Henderson, R., McLachlan, A. D., & Wallace, B. A. (1980) *Proc. Natl. Acad. Sci. U.S.A. 77*, 2023–2027.

Fiske, C. H., & Subbarow, Y. (1925) *J. Biol. Chem. 66*, 375–400.

Gordon, D. J., & Holzworth, G. (1971) *Arch. Biochem. Biophys. 142*, 481–488.

Henderson, R. (1975) *J. Mol. Biol. 93*, 123–138.

Henderson, R., & Unwin, P. N. T. (1975) *Nature (London) 257*, 28–32.

Hennessey, J. P., & Johnson, W. C. (1982) *Anal. Biochem. 125*, 177–188.

Heyn, M. P., Cherry, R. J., & Dencher, N. A. (1981) *Biochemistry 20*, 840–849.
Himmelblau, D. M. (1972) *Applied Nonlinear Programming*, p 341, McGraw-Hill, New York.
Jap, B. K., Maestre, M. F., Hayward, S. B., & Glaeser, R. M. (1983) *Biophys. J. 43*, 81–89.
Kendrew, J. G. (1962) *Brookhaven Symp. Biol. No. 15*, 215–226.
Kendrew, J. G., Dickerson, R. E., Strandberg, B. E., Hart, R. G., Davies, D. R., Philips, D. C., & Shore, V. C. (1960) *Nature (London) 185*, 422–427.
Leifer, D., & Henderson, R. (1983) *J. Mol. Biol. 163*, 451–466.
Lewis, B. A., & Engelman, D. M. (1983) *J. Mol. Biol. 166*, 203–210.
Long, M. M., Urry, D. W., & Stoeckenius, W. (1977) *Biochem. Biophys. Res. Commun. 75*, 725–731.
Lowry, O. H., Rosebrough, N. J., Farr, A. L., & Randall, R. J. (1951) *J. Biol. Chem. 193*, 265–275.
Magar, M. E. (1968) *Biochemistry 7*, 617–620.
Mao, D. (1984) Ph.D. Thesis, Columbia University.
Mao, D., Wachter, E., & Wallace, B. A. (1982) *Biochemistry 21*, 4960–4968.
Oesterhelt, D., & Stoeckenius, W. (1971) *Nature (London) 233*, 149–152.
Provencher, S. W., & Glöckner, J. (1981) *Biochemistry 20*, 33–37.
Racker, E. (1973) *Biochem. Biophys. Res. Commun. 55*, 224–230.
Rehorek, M., & Heyn, M. P. (1979) *Biochemistry 18*, 4977–4983.
Reich, C., Maestre, M. F., Edmondson, S., & Gray, D. M. (1980) *Biochemistry 19*, 5208–5213.
Reynolds, J. A., & Stoeckenius, W. (1977) *Proc. Natl. Acad. Sci. U.S.A. 74*, 2803–2804.
Schneider, A. S., & Harmatz, D. (1976) *Biochemistry 15*, 4158–4162.
Urry, D. W. (1972) *Biochim. Biophys. Acta 265*, 115–168.
Wallace, B. A., Kohl, N., & Teeter, M. M. (1984) *Proc. Natl. Acad. Sci. U.S.A. 81*, 1406–1410.

Identification of a Neutral Flavin Radical and Characterization of a Second Chromophore in *Escherichia coli* DNA Photolyase†

Marilyn Schuman Jorns,* Gwendolyn B. Sancar, and Aziz Sancar

ABSTRACT: DNA photolyase from *Escherichia coli* is a blue protein exhibiting absorption maxima at 580, 475, and 384 nm. One of the two chromophores present in this enzyme has been identified as the blue neutral flavin adenine dinucleotide (FAD) radical on the basis, in part, of visible absorption and electron spin resonance (ESR) data. The enzyme-bound radical ($\epsilon_{580} = 3.6 \times 10^3$ M^{-1} cm^{-1}) is stable toward O_2 or $K_3Fe(CN)_6$, is reversibly reduced by dithionite, and is converted to oxidized FAD upon aerobic denaturation. Disproportionation of the radical is observed upon anaerobic denaturation, consistent with an N-5 unsubstituted radical. The absorbance of the enzyme at $\lambda > 500$ nm is due only to the FAD radical whereas the band at 384 nm reflects contributions from both the radical and a second chromophore. The latter is labile when protein free at neutral pH ($\lambda_{max} = 360$ nm, $k = 5.5 \times 10^{-2}$ $min^{-1} \pm O_2$), a reaction that is readily monitored by the loss of an intense absorption band at 360 nm following enzyme denaturation under conditions where radical oxidation is immediate. This decomposition is pH dependent and the chromophore is stable at acid pH. Native photolyase is fluorescent (emission $\lambda_{max} = 470$ nm, excitation $\lambda_{max} = 398$ nm). An unlikely fluorescent flavin radical can be excluded by the position of the emission maximum. The enzyme fluorescence is attributed to the second chromophore.

Ultraviolet light causes formation of cyclobutane dimers between adjacent pyrimidine bases in DNA. The reaction, which can cause mutation, cancer, and death (Harm, 1981), is photochemically reversible. The dimer absorbs at shorter wavelengths that favor monomer formation while dimer formation is favored at longer wavelengths (Rupert, 1962) (eq 1). Action spectra observed for DNA photolyase vary

$$\text{Py} + \text{Py} \underset{240\text{ nm}}{\overset{280\text{ nm}}{\rightleftharpoons}} \text{Py–Py} \qquad (1)$$

somewhat depending on the source, but all exhibit maxima in the near-UV or visible region [418 nm, *Anacystis nidulans* (Saito & Werbin, 1970); 366 nm, yeast (Rupert & To, 1976); 360–380 nm, *Escherichia coli* (Jagger & Latarjet, 1956; Setlow, 1966); 400 nm, human (Sutherland et al., 1974); 435 nm, *Streptomyces griseus* (Jagger et al., 1969)]. Since direct excitation of pyrimidine dimers does not occur with near-UV or visible light, it has been proposed that the reaction might be a photosensitized process involving an enzyme-bound chromophore that absorbs in the near-UV or visible region. This hypothesis has not been easy to evaluate since DNA photolyase is usually present in very low levels in cells and isolation of even very modest amounts of enzyme has required heroic efforts. Nevertheless, Eker and his co-workers (Eker et al., 1981) recently showed that the enzyme from *S. griseus* does contain a chromophore that was identified as an 8-hydroxy-5-deazaflavin derivative. Studies with yeast DNA photolyase I (one of two photorepair enzymes present in this organism) show that FAD[1] is released when the enzyme is

† From the Department of Biological Chemistry, Hahnemann University School of Medicine, Philadelphia, Pennsylvania 19102 (M.S.J.), and the Department of Biochemistry, University of North Carolina School of Medicine, Chapel Hill, North Carolina 27514 (G.B.S. and A.S.). *Received January 26, 1984.* This work was supported in part by Grants GM 31704 (M.S.J.) and GM 31082 (A.S.) from the National Institutes of Health.

0006-2960/84/0423-2673$01.50/0